Electromagnetic fluctuations near thin metallic films

Luke S. Langsjoen, Amrit Poudel, Maxim G. Vavilov, and Robert Joynt
Department of Physics, University of Wisconsin, Madison, Wisconsin 53706, USA
(Received 22 October 2013; revised manuscript received 26 January 2014; published 3 March 2014)

We compute the electromagnetic fluctuations due to evanescent-wave Johnson noise in the vicinity of a thin conducting film, such as a metallic gate or a two-dimensional electron gas. This noise can decohere a nearby qubit, and it is also responsible for heat transfer and Casimir forces. We have improved on previous calculations of decoherence rates by including the nonlocal dielectric response of the film, which is an important correction at short distances. Remarkably, the fluctuations responsible for decoherence of charge qubits from a thin film are greatly enhanced over those arising from a conducting half space. The decoherence times can be reduced by over an order of magnitude by decreasing the film thickness. This appears to be due to the leakage into the vacuum of modes that are well localized in the perpendicular direction. There is no corresponding effect for spin qubits (magnetic field fluctuations). We also show that a nonlocal dielectric function naturally removes the divergence in the Casimir force at vanishing separation between two metallic sheets or half spaces. In the separation regime where local and nonlocal treatments are noticeably distinct, the Casimir attraction between two thin sheets and two half spaces is practically indistinguishable for any physical film thickness.

DOI: 10.1103/PhysRevB.89.115401 PACS number(s): 73.23.−b, 72.70.+m, 03.70.+k

I. INTRODUCTION

Thin metallic films are being used in an increasing number of nanotechnological applications. Semiconductor qubit architectures use conducting gates to isolate, manipulate, and read the qubit. While these conducting device elements are essential to the functionality of the qubit, they also give rise to an inevitable source of decoherence through evanescent-wave Johnson noise (EWJN) [1]. The top gates in accumulation-mode qubit architectures in particular are well approximated by a thin metallic film, and an accurate calculation of the decoherence times in these devices will require a detailed treatment of the electromagnetic properties of the films [2]. Thin films can also supply a desired or undesired source of heat transfer in micromechanical devices, and free-standing conducting films will experience stiction forces from nearby device elements through the Casimir effect.

The magnitude of heat transfer, the Casimir effect, and the qubit decoherence rate can all be obtained once the reflection coefficients of the film, r_p and r_s, have been calculated. r_p is the reflection coefficient for incident light with an electric field that is polarized in the plane of incidence, while r_s has its electric field polarized perpendicular to the incident plane.

In this paper we present a detailed derivation of these coefficients for the case of a general nonlocal dielectric function and use them to obtain quantitative calculations of the effects mentioned above. The thin-film reflection coefficients are found to exhibit important differences compared to a half space. These same nonlocal reflection coefficients have been found previously by Jones *et al.* [3] in the context of the anomalous skin effect and were used by Esquivel-Sirvent and Svetovoy [4] to obtain an expression for the Casimir force equivalent to that obtained here. The main contributions of the present work are to use these reflection coefficients to calculate decoherence rates of charge and spin qubits and to unify the formalisms describing qubit decoherence, heat transfer, and the Casimir effect for thin conducting films with a nonlocal dielectric response. Of central importance is our result that a nonlocal treatment removes all divergences in the size of these effects as the surface of the film is approached.

This paper is organized as follows. In Sec. II we derive our expression for the reflection coefficients of a thin film in a nonlocal treatment. In Secs. III and IV we then apply these coefficients to give a quantitative analysis of qubit decoherence from EWJN and stress-energy-tensor related phenomena, respectively. Section V shows how our reflection coefficients reduce to the cases of a local response and a conducting half space when the appropriate limits are taken. Finally, in Sec. VI we present our conclusions.

II. DERIVATION

We consider an infinite metallic sheet with nonlocal dielectric response whose surfaces are located at $z = -a$ and $z = 0$. To derive the reflection coefficients, we generalize the treatment by Ford and Weber [5] of a half space in the semiclassical infinite barrier model. The fields inside the sheet satisfy Maxwell's equations, and we consider fields varying harmonically in time at frequency ω, $\mathbf{E}(\mathbf{r},t) = \mathbf{E}(\mathbf{r})e^{-i\omega t}$. If we define the Fourier modes of all field quantities as $\mathbf{E}(\mathbf{r}) = \int d\mathbf{k}\mathbf{E}(\mathbf{k})\exp(i\,\mathbf{k}\cdot\mathbf{r})/(2\pi)^3$, etc., a general nonlocal dielectric function will relate $\mathbf{D}$ and $\mathbf{E}$ by

$$\mathbf{D}(\mathbf{k}) = \epsilon_l(k,\omega)\hat{\mathbf{k}}\cdot\mathbf{E}(\mathbf{k})\hat{\mathbf{k}} + \epsilon_t(k,\omega)[\mathbf{E}(\mathbf{k}) - \hat{\mathbf{k}}\cdot\mathbf{E}(\mathbf{k})\hat{\mathbf{k}}], \quad (1)$$

where we have separated the dielectric function into its longitudinal, ϵ_l, and transverse, ϵ_t, components. The reflection coefficients may be found through the surface impedances [6], defined as

$$Z^P(p,\omega) = -\frac{1}{\epsilon_0 c^2}\left\{\frac{\hat{\mathbf{p}}\cdot\mathbf{E}}{\hat{\mathbf{z}}\times\hat{\mathbf{p}}\cdot\mathbf{B}}\right\}_{\text{inside}},$$
$$Z^S(p,\omega) = \frac{1}{\epsilon_0 c^2}\left\{\frac{\hat{\mathbf{z}}\times\hat{\mathbf{p}}\cdot\mathbf{E}}{\hat{\mathbf{p}}\cdot\hat{\mathbf{B}}}\right\}_{\text{inside}}, \quad (2)$$

where $\hat{\mathbf{p}}$ is a unit vector along the direction of the in-plane component of the wave vector, and the fields are evaluated at the inner surface of the metal. The reflection coefficients may

then be written as

$$r_p = \frac{q_1/\epsilon_1 - Z^P\epsilon_0\omega}{q_1/\epsilon_1 + Z^P\epsilon_0\omega}, \quad r_s = \frac{Z^S\epsilon_0 c^2 - \omega/q_1}{Z^S\epsilon_0 c^2 + \omega/q_1}. \tag{3}$$

In the semiclassical infinite barrier model, it is assumed that the conduction electrons exhibit specular reflection at the boundary. In this model, the behavior of the fields inside a conducting half space are indistinguishable from the fields inside an infinite conductor with a current sheet at the location of the surface,

$$\mathbf{j}(\mathbf{r},t) = \mathbf{J}\delta(z)e^{i(\mathbf{p}\cdot\boldsymbol{\rho}-\omega t)}, \quad \hat{z}\cdot\mathbf{J} = 0, \tag{4}$$

where $\boldsymbol{\rho}$ is the position vector in the plane of the boundary, not to be confused with the electron density, and p is the component of the photon wave vector in the plane of the half space. For our case of a thin conducting film, the single current sheet is replaced by an infinite series of image current sheets:

$$\mathbf{j}(\mathbf{r},t) = \sum_{n=-\infty}^{\infty}\{\mathbf{J}_1\delta(z-2an) + \mathbf{J}_2\delta[z-a(2n+1)]\}e^{i(\mathbf{p}\cdot\boldsymbol{\rho}-\omega t)},$$
$$\hat{z}\cdot\mathbf{J}_1 = 0, \quad \hat{z}\cdot\mathbf{J}_2 = 0,$$

where $\mathbf{J}_1$ and $\mathbf{J}_2$, which correspond to images of the right and left surface current sheets, respectively, must be of equal magnitude and either parallel or antiparallel. Plugging this current source into Maxwell's equations allows us to solve for the electric and magnetic fields inside the metal,

$$\mathbf{E}(z) = \frac{2\pi}{i\omega a}\sum_{n=-\infty}^{\infty}\left[\left(\frac{\mathbf{J}_1 - (\mathbf{k}\cdot\mathbf{J}_1)\mathbf{k}/k^2}{\epsilon_t - c^2k^2/\omega^2} + \frac{(\mathbf{k}\cdot\mathbf{J}_1)\mathbf{k}}{k^2\epsilon_l}\right) + (-1)^n\left(\frac{\mathbf{J}_2 - (\mathbf{k}\cdot\mathbf{J}_2)\mathbf{k}/k^2}{\epsilon_t - c^2k^2/\omega^2} + \frac{(\mathbf{k}\cdot\mathbf{J}_2)\mathbf{k}}{k^2\epsilon_l}\right)\right]e^{iqz},$$
$$\mathbf{B}(z) = \frac{2\pi c}{i\omega^2 a}\sum_{n=-\infty}^{\infty}\left(\frac{\mathbf{k}\times\mathbf{J}_1}{\epsilon_t - c^2k^2/\omega^2} + \frac{(\mathbf{k}\times\mathbf{J}_2)(-1)^n}{\epsilon_t - c^2k^2/\omega^2}\right)e^{iqz}. \tag{5}$$

It can be seen by inspection that $\mathbf{J}_1 = \mathbf{J}_2$ corresponds to field components whose wavelength in the z direction is an integer fraction of the thickness a, while $\mathbf{J}_1 = -\mathbf{J}_2$ corresponds to wavelengths in the z direction that are half-integer fractions of a. Comparison to Ford and Weber shows that the fields within a thin film differ from those within a half space by replacing the integral over a continuous q by a summation over a discrete $q_n = 2n\pi/a$ or $q_n = (2n+1)\pi/a$ depending on whether $\mathbf{J}_1 = \mathbf{J}_2$ or $\mathbf{J}_1 = -\mathbf{J}_2$, respectively. The reflection coefficients are then obtained by summing the contribution from both cases.

$$r_p = \frac{1}{2}\sum_{i=e,o}\frac{1 - \frac{2i}{\kappa a}\sum_{n=-\infty}^{\infty}F_p(k_i,\omega)}{1 + \frac{2i}{\kappa a}\sum_{n=-\infty}^{\infty}F_p(k_i,\omega)}, \tag{6}$$

$$r_s = \frac{1}{2}\sum_{i=e,o}\frac{1 + \frac{2i\kappa c^2}{a\omega^2}\sum_{n=-\infty}^{\infty}F_s(k_i,\omega)}{-1 + \frac{2i\kappa c^2}{a\omega^2}\sum_{n=-\infty}^{\infty}F_s(k_i,\omega)}, \tag{7}$$

$$F_p(k,\omega) \equiv \frac{1}{k^2}\left(\frac{q^2}{\epsilon_t(k,\omega) - c^2k^2/\omega^2} + \frac{p^2}{\epsilon_l(k,\omega)^2}\right), \tag{8}$$

$$F_s(k,\omega) \equiv \frac{1}{\epsilon_t(k,\omega) - c^2k^2/\omega^2}, \tag{9}$$

where $\kappa^2 = \omega^2/c^2 - p^2$, $q_e = 2n\pi/a$, $q_o = (2n+1)\pi/a$, $k_e^2 = p^2 + q_e^2$, and $k_o^2 = p^2 + q_o^2$. While expressions (6) and (7) are valid for a general nonlocal dielectric response, for all numerical results presented in this paper we use the Lindhard forms

$$\epsilon_l(k,\omega) = 1 + \frac{3\omega_p^2}{k^2v_F^2}\frac{(\omega+i\nu)f_l[(\omega+i\nu)/kv_F]}{\omega+i\nu f_l[(\omega+i\nu)/kv_F]}, \tag{10a}$$

$$\epsilon_t(k,\omega) = 1 - \frac{\omega_p^2}{\omega(\omega+i\nu)}f_t[(\omega+i\nu)/kv_F], \tag{10b}$$

$$f_l(x) = 1 - \frac{x}{2}\ln\left(\frac{x+1}{x-1}\right), \tag{11a}$$

$$f_t(x) = \frac{3}{2}x^2 - \frac{3}{4}x(x^2-1)\ln\left(\frac{x+1}{x-1}\right). \tag{11b}$$

Here ν is the electron collision frequency, $\omega_p = (4\pi ne^2/m)^{1/2}$ is the plasma frequency, and v_F is the Fermi velocity. For all results presented in this paper, we use the values $\nu = 4\pi c \times 10^4$ s^{-1}, $\omega_p = 1.6\times10^{16}$ s^{-1}, and $\lambda_F \equiv h/m_e v_F = 0.4$ nm. This derivation runs closely parallel to that of Jones *et al.* [3] and Esquivel-Sirvent and Svetovoy [4]. In the following sections we will apply Eqs. (6) and (7) to a variety of physical systems.

III. DECOHERENCE

A. Energy relaxation

Here we present a quantitative comparison of the relaxation times of a point-charge or spin qubit when exposed to a conducting half space or thin film in both local and nonlocal treatments. The relaxation rate for a charge or spin qubit is proportional to the spectral density of the fluctuating electric or magnetic field, respectively, at the location of the qubit. Quantitatively, for a charge qubit of electric dipole moment d or a spin qubit of magnetic dipole moment μ pointing in the ith direction at position $\mathbf{r}$ with level separation ω_Z, we have

$$\frac{1}{T_{1,c}} = \frac{d^2}{\hbar^2}\chi_{ii}^E(\vec{r},\vec{r},\omega_Z)\coth\left(\frac{\hbar\omega_Z}{2k_BT}\right), \tag{12}$$

$$\frac{1}{T_{1,s}} = \frac{\mu^2}{\hbar^2}\chi_{ii}^B(\vec{r},\vec{r},\omega_Z)\coth\left(\frac{\hbar\omega_Z}{2k_BT}\right), \tag{13}$$

where $\chi_{ii}^{E,B}(\vec{r},\vec{r},\omega_Z)$ are the electric and magnetic spectral densities, respectively, and $\vec{r}$ is the location of the qubit [7]. The spectral densities are given by an integral expression involving the reflection coefficients. We pause to emphasize that the temperature dependence of the relaxation rates is entirely determined by the Planck function. If we take the qubit to point along the z direction, perpendicular to the surface, the relevant components of the spectral density tensors are

$$\chi_{zz}^E(z,z,\omega) = \hbar\mathrm{Re}\int_0^\infty\frac{p^3}{q}dpe^{2iqz}r_p(p), \tag{14}$$

$$\chi_{zz}^B(z,z,\omega) = \frac{\hbar}{c^2}\mathrm{Re}\int_0^\infty\frac{p^3}{q}dpe^{2iqz}r_s(p), \tag{15}$$

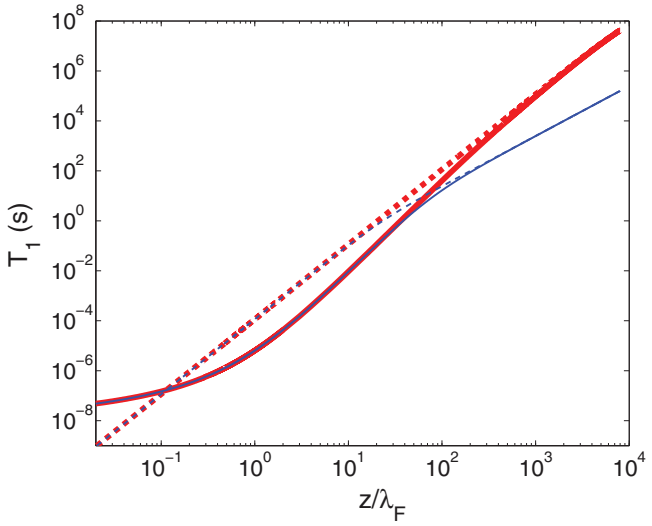

FIG. 1. (Color online) T_1 time of a point-charge qubit oriented along the z axis as a function of distance from the conductor, expressed in units of the Fermi wavelength, $\lambda_F = 0.4$ nm. Dashed and solid lines indicate local and nonlocal dielectric responses, respectively, for a half space (thick red lines) and a thin film of thickness $a =$ 10 nm (thin blue lines). The local results are seen to diverge as $1/z^3$ as $z \to 0$.

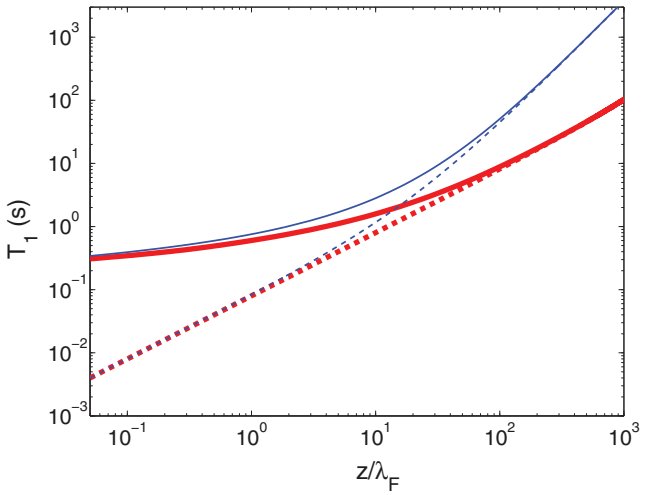

FIG. 2. (Color online) T_1 time of a point spin qubit oriented along the z axis as a function of distance from the conductor, expressed in units of the Fermi wavelength, $\lambda_F = 0.4$ nm. Dashed and solid lines indicate local and nonlocal dielectric responses, respectively, for a half space (thick red lines) and a thin film of thickness $a = 10$ nm (thin blue lines). The local results are seen to diverge as $1/z$ as $z \to 0$.

where q is the z-component of the photon wavevector and p is the transverse component; $q = \sqrt{\omega^2/c^2 - p^2}$ for $p^2 \leqslant \omega^2/c^2$ and $q = i\sqrt{p^2 - \omega^2/c^2}$ for $p^2 > \omega^2/c^2$.

Figure 1 shows the T_1 time for a charge qubit oriented along the z axis as a function of distance from the conductor. T_1 times for a charge qubit oriented along other directions are qualitatively unchanged. Our primary result, T_1 from a thin film with a nonlocal dielectric function, is given by the solid blue curve. Of particular note are its convergence to the nonlocal half-space result as $z \to 0$ and its convergence to the local thin-film result for large z. For intermediate distances the nonlocal field fluctuations are enhanced above those given by a local treatment, while for smaller distances they converge to a finite value while the local result diverges as $1/z^3$. This inversion has been noted before by Volokitin and Persson in the context of heat transfer [8] and may be understood as follows. Increasing the separation between the conducting surface and the qubit changes the wavelength of the electromagnetic field that predominantly contributes to relaxation. This dominant wavelength will increase with the separation, as the shorter wavelengths are exponentially suppressed more strongly. As the dominant wavelength crosses over the mean free path of the metal, a nonlocal treatment will give an enhanced spectrum because of a commensurability between the electromagnetic field and the response of the electron system. Electromagnetic field fluctuations with a wavelength much smaller than the mean free path are suppressed in a nonlocal treatment, causing the fluctuating field strength to cross over the local result and converge to a finite value as the separation vanishes, as seen in Fig. 1.

Also, for separations $z > 10\lambda_F$ the electric-field fluctuations outside a thin film are noticeably enhanced relative to those outside a half space. This enhancement can be understood by analogy to a quantum particle trapped in a finite square well. Further squeezing of the particle will lead to increased leakage of the wave function into the forbidden region. The distinction between the half-space and thin-film fluctuations vanishes as $z \to 0$. Figure 2 shows comparable results for a spin qubit oriented along the z axis, which will relax from fluctuations of the magnetic field. A local treatment of magnetic field fluctuations exhibits a weaker $1/z$ divergence. The enhancements of the nonlocal over the local field strength and of the thin film over the half space are not present for the magnetic case.

B. Dephasing

In this section we present results for the pure dephasing time of a charge or spin qubit from EWJN near a thin film. The dephasing rate may be found through an examination of the off-diagonal elements of the time-dependent density matrix [9]. We assume initially that dephasing dominates over energy relaxation, and so we consider qubit-environment coupling which is diagonal in the energy eigenbasis of the qubit. Following [10], our Hamiltonian takes the form

$$H = H_s + H_b + H_i = \frac{1}{2}\sigma_z\omega_z + \sum_k \omega_k a_k^\dagger a_k + \Lambda_s \sum_k (g_k^* a_k + g_k a_k^\dagger), \qquad (16)$$

where H_s is the two-level system Hamiltonian of the qubit, H_b is the bath Hamiltonian for the fluctuating field, and H_i represents the system-bath interaction. $a_k^\dagger$ and a_k are creation and annihilation operators, respectively, for field modes with wave vector k. Λ_s is the coupling strength of the system observable to the fluctuating environment, and g_k is the coupled field quantity with mode k. In our case, Λ_s will always be proportional to σ_z in the pseudospin eigenbasis of the qubit. Because H_i then commutes with H_s, our model will not describe energy relaxation. For the case of a charge qubit, the creation and annihilation operators are for electric-field

modes, while for a spin qubit, we have magnetic field creation and annihilation operators. For a charge qubit $\Lambda_s = d\sigma_z$, while for a spin qubit $\Lambda_s = \mu\sigma_z$, where d and μ are the electric and magnetic dipole moments, respectively. If we take the qubit to point in the ith direction, $g_k = E_{k,i}$ for a charge qubit, where $E_{k,i}$ is the ith component of an electric-field fluctuation with wave vector k, while $g_k = B_{k,i}$ for a spin qubit, where $B_{k,i}$ is the corresponding component of the magnetic field.

As shown in Ref. [10], the time dependence of the off-diagonal components of the reduced density matrix can be written as

$$\rho_{01}(t) = \rho_{01}(0)e^{-\Gamma(t)}, \tag{17}$$

where for a two-level system

$$\Gamma(t) = \frac{1}{2\hbar^2}\sum_k \frac{|g_k|^2}{\omega_k^2}\sin^2\frac{\omega_k t}{2}\coth\frac{\hbar\omega_k}{2k_BT}. \tag{18}$$

The density matrix has been reduced in the sense of taking a thermal and quantum average over the bath degrees of freedom. This allows $|g_k|^2$ to be expressed in terms of the electric and magnetic spectral densities, defined in Sec. III A. The dephasing time T_ϕ is then defined as the value of t for which $\Gamma(t) = 1$.

A realistic qubit system will experience both pure dephasing and energy relaxation. In this case the system-bath interaction Hamiltonian will contain terms proportional to σ_x as well as σ_z in the pseudospin basis. It is a well-known result [11] that the dephasing time T_2 is then given by a reciprocal sum of contributions from energy relaxation and pure dephasing:

$$\frac{1}{T_2} = \frac{1}{2T_1} + \frac{1}{T_\phi}, \tag{19}$$

where T_1 is given in Sec. III A.

Results for pure dephasing times of charge and spin qubits oriented in the z direction as a function of separation from the film are shown in Figs. 3 and 4, respectively. Dephasing times are qualitatively unchanged from and are of the same order of magnitude as qubit relaxation times. This can be understood because EWJN is characterized by Ohmic, rather than $1/f$, noise, and it is does not exhibit an enhancement from the low-frequency part of the spectrum.

IV. STRESS-ENERGY TENSOR

In this section we present results for two closely related phenomena that are proportional to the stress-energy tensor in the vicinity of the conducting film.

A. Heat transfer

The problem of heat transfer between conducting half spaces with a nonlocal dielectric function has been treated in depth by Chapuis *et al.* [12]. They show that magnetic field fluctuations, governed primarily by the r_s coefficient, supply the dominant contribution to heat transfer between metallic surfaces at short distances ($d < 10^{-7}$ m). The local expression for r_s does not lead to a divergent heat transfer rate at zero separation, so they argue that the nonlocal corrections may be safely ignored for half spaces. We anticipate that the result for thin films will be qualitatively similar.

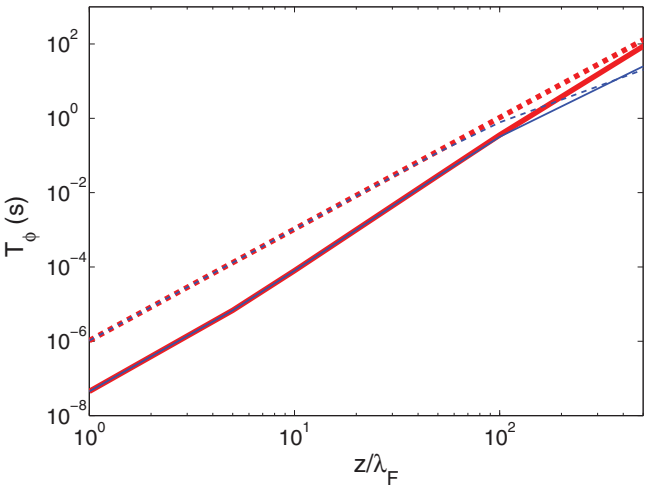

FIG. 3. (Color online) T_ϕ time of a point-charge qubit oriented along the z axis as a function of distance from the conductor, expressed in units of the Fermi wavelength, $\lambda_F = 0.4$ nm. Dashed and solid lines indicate local and nonlocal dielectric responses, respectively, for a half space (thick red lines) and a thin film of thickness $a = 50$ nm (thin blue lines). Here we take temperature $T = 1$ K. The crossover between the local and nonlocal result is not seen here because the z axis only extends down to $\sim\lambda_F$.

Heat flux from one surface to another will be proportional to the value of the Poynting vector in the direction of their separation at the location of the second surface. We will thus be interested in the ensemble average of

$$\langle \mathbf{S}(\mathbf{r})\rangle_\omega = \frac{c}{8\pi}[\langle \mathbf{E}(\mathbf{r})\times\mathbf{B}^*(\mathbf{r})\rangle_\omega + \langle \mathbf{E}^*(\mathbf{r})\times\mathbf{B}(\mathbf{r})\rangle_\omega]. \tag{20}$$

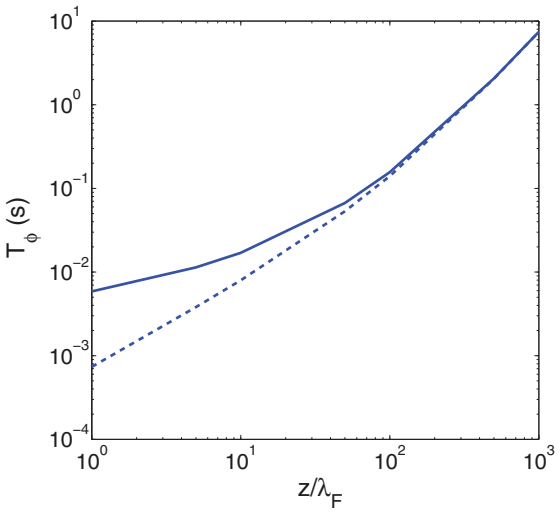

FIG. 4. (Color online) T_ϕ time of a point spin qubit oriented along the z axis as a function of distance from the conductor, expressed in units of the Fermi wavelength, $\lambda_F = 0.4$ nm. Blue dashed and solid lines indicate local and nonlocal dielectric responses, respectively, for a thin film of thickness $a = 50$ nm. Here we take temperature $T = 1$ K.

Volokitin [8] found, for the case of two parallel semi-infinite bodies with separation z and reflection coefficients r_{s1},r_{p1},r_{s2}, and r_{p2},

$$S_z = \hbar\omega \int_0^\infty \frac{d\omega}{2\pi}[N_1(\omega) - N_2(\omega)]\left(4\int_{q>\omega/c} \frac{d^2q}{(2\pi)^2} e^{-2|k|z} \times \frac{\mathrm{Im}r_{p1}(\mathbf{q},\omega)\mathrm{Im}r_{p2}(\mathbf{q},\omega)}{[1-e^{-2|k|z}r_{p1}(\mathbf{q},\omega)r_{p2}(\mathbf{q},\omega)]^2} + [p \to s]\right), \quad (21)$$

where $[p \to s]$ denotes replacing the coefficients r_p with r_s and $N_{1,2}$ represent the Planck functions for the left and right films, respectively,

$$N_i(\omega) = (e^{\hbar\omega/k_B T_i} - 1)^{-1}. \quad (22)$$

In Eq. (21) we have dropped the lower portion of the integral over q when $q < \omega/c$. This part of the spectrum represents the radiative blackbody contribution to heat transfer, which is negligibly small compared to the evanescent-wave contribution. At a separation of 30 nm, the propagating part will give a significant contribution only for extremely high frequencies, $\omega > 10^{15}$ Hz [12]. These fluctuations will be suppressed by the Boltzmann factor. If Eqs. (26) and (27) are plugged into Eq. (21), a $1/z^2$ divergence in the heat transfer rate will emerge. The nonlocal reflection coefficients for a thin film, Eqs. (6) and (7), vanish for sufficiently large wave vectors $q > 1/\lambda_F$, which will remove this divergence to give a finite heating rate at zero separation. The results of Chapuis *et al.* [12] may be recovered by using expressions (24) and (25) in Eq. (21). For a more detailed discussion of heat transfer from a material with a nonlocal dielectric response, we refer the interested reader to their paper.

B. Casimir effect

It is instructive to see how the inclusion of nonlocal dielectric properties affects the Casimir attraction between two parallel thin metallic films. The Casimir interaction between thin films has been studied previously by several authors. Yampol'skii *et al.* investigated the temperature dependence of the Casimir attraction between thin conducting films [13]. They discovered the possibility of a nonmonotonic temperature dependence of the force due to a competition between the decrease in conductivity and the increase in available thermal modes with increasing temperature. Boström *et al.* calculated the attractive force between atomically thin gold films, using density functional theory to derive the anisotropic deviations of the dielectric function of a thin film from its value in a bulk conductor [14]. They found that the more accurate anisotropic dielectric function gives an enhanced attractive force relative to what is obtained using the bulk dielectric function. The force, however, is still suppressed compared to the force between gold half spaces. In both of these papers, the treatment of the dielectric function was local and led to the usual unphysical divergence of the Casimir force at vanishing separation. Esquivel and Svetovoy derive an expression for the Casimir force between half spaces [15] and thin films [4] equivalent to ours. They find that the nonlocal correction to the force between thin films is more significant than it is for half spaces, although these corrections are still less than a percent for a separation of 50 nm. Our only supplement to their work is to emphasize that the nonlocal treatment removes the unphysical divergence of the force at zero separation.

To calculate the Casimir force per area between thin films with a nonlocal response, we use the generalization of the Lifshitz formula derived by Mochán [16]:

$$\frac{F(L)}{A} = \frac{\hbar c}{2\pi^2}\int_0^\infty dQ\,Q \int_{q\geqslant 0} dk \frac{\tilde{k}^2}{q} \times \mathrm{Re}\left(\frac{r_{s1}r_{s2}e^{2i\tilde{k}L}}{1-r_{s1}r_{s2}e^{2i\tilde{k}L}} + \frac{r_{p1}r_{p2}e^{2i\tilde{k}L}}{1-r_{p1}r_{p2}e^{2i\tilde{k}L}}\right). \quad (23)$$

Here $\tilde{k} = k + i0^+$, and the integral over k runs from iQ to 0 and then to ∞. The subscripts 1 and 2 on the reflection coefficients refer to the left and right surfaces, respectively. If the Fresnel reflection coefficients are plugged into Eq. (23), the original Lifshitz formula is recovered, but this expression is more generally applicable.

The Casimir forces per area between two thin films and two half spaces in both local and nonlocal treatments are shown in Fig. 5. A nonlocal treatment of the dielectric function is shown to naturally yield a finite force at zero separation for both thin films and half spaces, without having to use renormalization techniques or an external cutoff on high-frequency modes. The distinction between the Casimir attraction of thin films and half spaces is insignificant at separations that are sufficiently small to necessitate a nonlocal dielectric function. For larger separations we find the attraction between thin films is suppressed compared to the attraction between half spaces, consistent with previous work [4,14]. We pause to mention that at separations smaller than the Fermi wavelength, surface roughness effects and chemical attraction

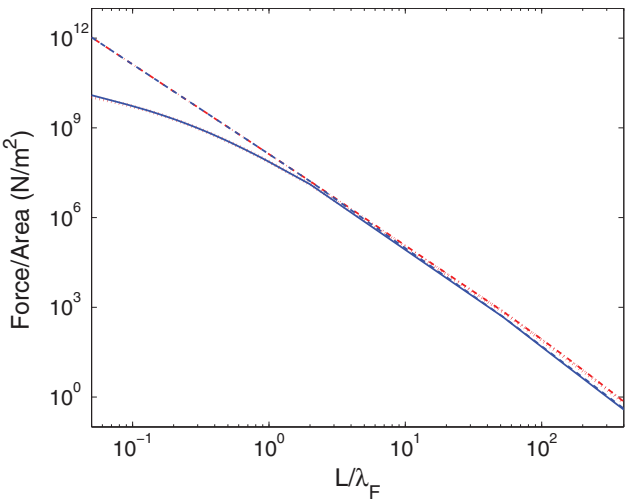

FIG. 5. (Color online) Plot of the Casimir force per area between two metallic plates as a function of their separation, in units of the Fermi wavelength, $\lambda_F = 0.4$ nm. Red dash-dotted and dotted lines indicate local and nonlocal dielectric responses, respectively, for two conducting half spaces, whereas blue dashed and solid lines indicate local and nonlocal dielectric responses for two thin films of thicknesses $a = 5$ nm each.

between the films will begin to challenge the validity of our quasimacroscopic approach to the problem [15].

V. LIMITING CASES

Including a nonlocal dielectric response alters the expressions for EWJN strength, the heat transfer rate, and the Casimir force solely through a modification of the reflection coefficients r_p and r_s. For completeness, we present here how Eqs. (6) and (7) reduce to their local and half-space counterparts when appropriate limits are taken.

Taking the limit $a \to \infty$ in Eqs. (6) and (7) eliminates the distinction between the even and odd summations by converting them both into an integral over a continuous q. Doing so gives the reflection coefficients for a metallic half space with a nonlocal dielectric response

$$r_p = \frac{1 - \frac{2i}{\pi\kappa}\int_0^\infty \frac{dq}{k^2}\left(\frac{q^2}{\epsilon_t(k,\omega)-c^2k^2/\omega^2} + \frac{p^2}{\epsilon_l(k,\omega)^2}\right)}{1 + \frac{2i}{\pi\kappa}\int_0^\infty \frac{dq}{k^2}\left(\frac{q^2}{\epsilon_t(k,\omega)-c^2k^2/\omega^2} + \frac{p^2}{\epsilon_l(k,\omega)^2}\right)}, \tag{24}$$

$$r_s = \frac{\frac{2i\kappa c^2}{\pi\omega^2}\int_0^\infty \frac{dq}{\epsilon_t(k,\omega)-c^2k^2/\omega^2} + 1}{\frac{2i\kappa c^2}{\pi\omega^2}\int_0^\infty \frac{dq}{\epsilon_t(k,\omega)-c^2k^2/\omega^2} - 1}, \tag{25}$$

where $k^2 = p^2 + q^2$. Alternatively, the reflection coefficients for a thin film with a local response can be obtained from Eqs. (6) and (7) by setting $\epsilon_t(k,\omega) = \epsilon_l(k,\omega) = \epsilon(\omega)$, where $\epsilon(\omega)$ is a local dielectric function that is independent of k. In this case the summations over n may be evaluated in closed form and give

$$r_p = \frac{1}{2}\left(\frac{\kappa\epsilon - i\kappa_1\cot(\kappa_1 a/2)}{\kappa\epsilon + i\kappa_1\cot(\kappa_1 a/2)} + \frac{\kappa\epsilon + i\kappa_1\tan(\kappa_1 a/2)}{\kappa\epsilon - i\kappa_1\tan(\kappa_1 a/2)}\right),$$

$$r_s = \frac{1}{2}\left(\frac{\kappa - i\kappa_1\cot(\kappa_1 a/2)}{\kappa + i\kappa_1\cot(\kappa_1 a/2)} + \frac{\kappa + i\kappa_1\tan(\kappa_1 a/2)}{\kappa - i\kappa_1\tan(\kappa_1 a/2)}\right),$$

where $\kappa_1^2 = \omega^2\epsilon/c^2 - p^2$. Combining the two terms yields the form given in Ref. [17]:

$$r_p = \frac{\epsilon^2\kappa^2 - \kappa_1^2}{\kappa_1^2 + \epsilon^2\kappa^2 + 2i\kappa\kappa_1\epsilon\cot(\kappa_1 a)}, \tag{26}$$

$$r_s = \frac{\kappa^2 - \kappa_1^2}{\kappa^2 + \kappa_1^2 + 2i\kappa\kappa_1\cot(\kappa_1 a)}. \tag{27}$$

Finally, setting $\epsilon_t(k,\omega) = \epsilon_l(k,\omega) = \epsilon(\omega)$ in Eqs. (24) and (25) or sending $a \to \infty$ in Eqs. (26) and (27) gives the traditional Fresnel reflection coefficients,

$$r_p = \frac{\epsilon\kappa - \kappa_1}{\epsilon\kappa + \kappa_1}, \quad r_s = \frac{\kappa - \kappa_1}{\kappa + \kappa_1}.$$

VI. CONCLUSIONS

We have presented a detailed microscopic treatment of the reflective properties of thin metallic films, where the use of a general nonlocal dielectric function has incorporated the discrete nature of the valence electrons inside the metal. The inclusion of nonlocality in the dielectric function removes a spurious divergence in the rate of heat transfer and the strengths of both EWJN and the Casimir attraction at zero separation from the film. This is accomplished through a suppression of the reflection coefficients for values of the transverse wave vector larger than the inverse of the Fermi wavelength. Uniquely, electric-field evanescent waves are enhanced in the nonlocal treatment for an intermediate range of distances on the order of the Fermi wavelength. This enhancement will lead to a decrease in the decoherence times of charge qubits below what would be expected from a local treatment. This comes about from an enhancement of r_p that is not present for r_s. Additionally, there is an enhancement of r_p for a thin film over that for a half space for all separations. Because the material is not magnetoactive, this enhancement is not present for magnetic field fluctuations, i.e., for r_s.

We expect the nonlocal corrections to the reflection coefficients to become more practically relevant in the future as micromechanical devices are further miniaturized. Beyond the use of metallic sheets in such devices, graphene has been popularized recently as a material in micromechanical devices because of its unique electromagnetic properties [18]. It would be interesting to see how the results presented here would generalize to the case of graphene. At present, decoherence times in contemporary qubit devices seem to be limited by EWJN only for spin qubits at low external magnetic field [17]. However, we expect EWJN to become a dominant source of decoherence in charge qubits in the future when other noise sources are more effectively suppressed.

ACKNOWLEDGMENTS

This work was funded by ARO and LPS Grant No. W911NF-11-1-0030. The views and conclusions contained in this document are those of the authors and should not be interpreted as representing the official policies, either expressly or implied, of the US government.

[1] C. Henkel, S. Pötting, and M. Wilkens, Appl. Phys. B **69**, 379 (1999).
[2] M. G. Borselli, K. Eng, E. T. Croke, B. M. Maune, B. Huang, R. S. Ross, A. A. Kiselev, P. W. Deelman, I. Alvarado-Rodriguez, A. E. Schmitz, M. Sokolich, K. S. Holabird, T. M. Hazard, M. F. Gyure, and A. T. Hunter, Appl. Phys. Lett. **99**, 063109 (2011).
[3] W. E. Jones, K. L. Kliewer, and R. Fuchs, Phys. Rev. **178**, 1201 (1969).
[4] R. Esquivel-Sirvent and V. B. Svetovoy, Phys. Rev. B **72**, 045443 (2005).
[5] G. W. Ford and W. H. Weber, Phys. Rep. **113**, 195 (1984).
[6] L. D. Landau and E. M. Lifshitz, *Electrodynamics of Continuous Media* (Pergamon, London, 1960), Vol. 8, Chap. X.
[7] L. S. Langsjoen, A. Poudel, M. G. Vavilov, and R. Joynt, Phys. Rev. A **86**, 010301 (2012).

[8] A. I. Volokitin and B. Persson, Rev. Mod. Phys. **79**, 1291 (2007).
[9] M. G. Palma, K. A. Suominen, and A. K. Ekert, Proc. R. Soc. London, Ser. A **452**, 567 (1996).
[10] D. Mozyrsky and V. Privman, J. Stat. Phys. **91**, 787 (1998).
[11] Yu. Makhlin, G. Schön, and A. Shnirman, in *New Directions in Mesoscopic Physics (Towards Nanoscience)*, edited by R. Fazio *et al*. (Kluwer, Dordrecht, 2003), pp. 197–224.
[12] P. O. Chapuis, S. Volz, C. Henkel, K. Joulain, and J. J. Greffet, Phys. Rev. B **77**, 035431 (2008).
[13] V. A. Yampol'skii, S. Savel'ev, Z. A. Mayselis, S. S. Apostolov, and F. Nori, Phys. Rev. Lett. **101**, 096803 (2008).
[14] M. Boström, C. Persson, and B. E. Sernelius, Eur. Phys. J. B **86**, 43 (2013).
[15] R. Esquivel and V. B. Svetovoy, Phys. Rev. A **69**, 062102 (2004).
[16] W. L. Mochán, Rev. Mex. Fis. **48**, 339 (2002).
[17] A. Poudel, L. S. Langsjoen, M. G. Vavilov, and R. Joynt, Phys. Rev. B **87**, 045301 (2013).
[18] R. Messina and P. Ben-Abdallah, Sci. Rep. **3**, 1383 (2013).